Journal of Systems Engineering and Electronics
Vol. 34, No. 1, February 2023, pp.19 – 27

Classification of birds and drones by exploiting periodical motions in Doppler spectrum series

DUAN Jia[1], ZHANG Lei[1], WU Yifeng[1], ZHANG Yue[1,*], ZHAO Zeya[2], and GUO Xinrong[3]

1. School of Electronics and Communication, Sun Yat-Sen University, Shenzhen 518107, China; 2. Beijing Institute of Tracking and Telecommunication Technology, Beijing 100854, China; 3. Armed Police Engineering University, Xi'an 510507, China

Abstract: With the rapidly growing abuse of drones, monitoring and classification of birds and drones have become a crucial safety issue. With similar low radar cross sections (RCSs), velocities, and heights, drones are usually difficult to be distinguished from birds in radar measurements. In this paper, we propose to exploit different periodical motions of birds and drones from high-resolution Doppler spectrum sequences (DSSs) for classification. This paper presents an elaborate feature vector representing the periodic fluctuations of RCS and micro kinematics. Fed by the Doppler spectrum and feature sequence, the long to short-time memory (LSTM) is used to solve the time series classification. Different classification schemes to exploit the Doppler spectrum series are validated and compared by extensive real-data experiments, which confirms the effectiveness and superiorities of the proposed algorithm.

Keywords: target classification, long-to-short memory (LSTM), drone discrimination, Doppler spectrum series.

DOI: 10.23919/JSEE.2023.000002

1. Introduction

The monitoring and recognition of drones have been a crucial safety issue nowadays, with the rapidly growing abuse of drones in criminal and antisocial activities [1−4]. Among the effective sensors for detecting small and slow-moving targets, radar is outstanding for all-weather day and night working conditions. However, the radar detection of drones inevitably introduces unwanted low-energy bird signals because of their similar radar cross sections (RCSs). Therefore, the classification problem of birds by radar and drones is crucial surveillance against drones. However, the discrimination of drones from birds by radar is difficult, as they share similar characteristics in radar measurements, such as low RCSs, similar velocities, and similar heights. Traditional classification methods degrade in recognizing these small targets since they require high resolutions to obtain scattering features and contour information for classification.

The three main feature classes are the micro-Doppler related features, the polarized related features, and the track related features. Available techniques for radar classification of birds and drones mainly consist of three main categories, depending on the target properties exploited. (i) Most available publications prefer to extract the micro-Doppler features to distinguish drones from birds. The repetitive wing beating pattern and rotor blade rotation introduce different modulation modes to the Doppler spectrum. These micro-Doppler features are robust features for classification [5−9]. However, it is challenging to capture the micro-Doppler signals of small targets for practical applications due to their low RCSs [10,11]. (ii) Researchers showed the potential of utilizing polarimetric scattering effects to classify birds and drones [12,13]. However, polarimetry increases the complexity of radar systems. (iii) Besides these features, track-related features contribute to the separation of birds and drones [14,15]. By constructing the kinematic features, the RCS-related features, and the track morphology features of the original track information, researchers validate the effectiveness of track feature-based classification of birds and drones. However, the errors of track-related features are different for different radar systems. Therefore, the subsequent sorting may degrade with varying radar systems. To conclude, the classification problem of birds and drones is a relatively novel and challenging topic for

Manuscript received April 07, 2022.
*Corresponding author.
This work was supported by the National Natural Science Foundation of China (62101603), the Shenzhen Science and Technology Program (KQTD20190929172704911), the Aeronautical Science Foundation of China (2019200M1001), the National Nature Science Foundation of Guangdong (2021A1515011979), the Guangdong Key Laboratory of Advanced IntelliSense Technology (2019B121203006), and the Pearl River Talent Recruitment Program (2019ZT08X751).

radars [16]. Theoretical and experimental research are insufficient, especially for the latter two kinds of classification methods.

In this paper, we use the high-resolution Doppler spectrum sequences (DSSs) to exploit both the periodic fluctuations of RCS and micro kinematics to classify birds and drones. It provides a more convenient means for classifying birds and drones with minor restrictions on radar systems. Firstly, it is independent of the detection of micro-Doppler signals. The micro kinematics of targets is defined by constructing an RCS centralized parameter whether micro-Doppler exhibits or not. Secondly, unlike the track feature-based method in [14], features are extracted from the DSS, which can be normalized to eliminate errors among different systems. Finally, by introducing long-short-time memory (LSTM), we explore different underlying periodical behaviors of birds and drones.

The main contributions of our proposal lie in exploiting the DSS to classify birds and drones for the first time by revealing their different periodical motions.

The remaining parts of our paper are organized as follows. Section 2 presents the handcrafted features constructed from DSS. Section 3 introduces the LSTM to classify birds and small drones. By illustrating the basis of LSTM, we propose the LSTM architectures for radar small target classification in detail. Experimental results and analysis round off real-measured data in Section 4. Section 4 also gives a detailed analysis of the effects of frame numbers, data varieties, and signal to noise ratios (SNRs) on proposals. Conclusions are presented in Section 5.

2. Feature vector construction of DSS

Unlike the track information in [14,15], only use relative Doppler and amplitude sequences are used for classification in this paper, namely, the DSS data, as Fig. 1 shows. It is a typical DSS image of a bird and a drone. The bright center line in Fig. 1 stands for ground clutter.

Table 1 summarizes the essential information in the Doppler spectrum at each frame. As Table 1 shows, relative speed, amplitude, and acceleration are typical physical features. The relative velocity v_i is defined as the ratio of the targets' velocity to the velocity resolution by finding the peak position in the ith DSS. The amplitude A_i is defined as the maximum value in the i th DSS. The acceleration means the speed difference. For example, $a_i = v_{i+1} - v_i$ with $a_1 = 0$. Since the micro-Doppler phenomenon introduces diffusions in the Doppler spectrum, we define N_i and S_i to depict the micromotion degree of the target, as shown in the zoomed picture in Fig. 1. N_i is the number of points of marks in the Doppler spectrum. Moreover, S_i is the sum of the amplitudes of these points. These parameters can be easily obtained by constant false alarm rate (CFAR) detection [17].

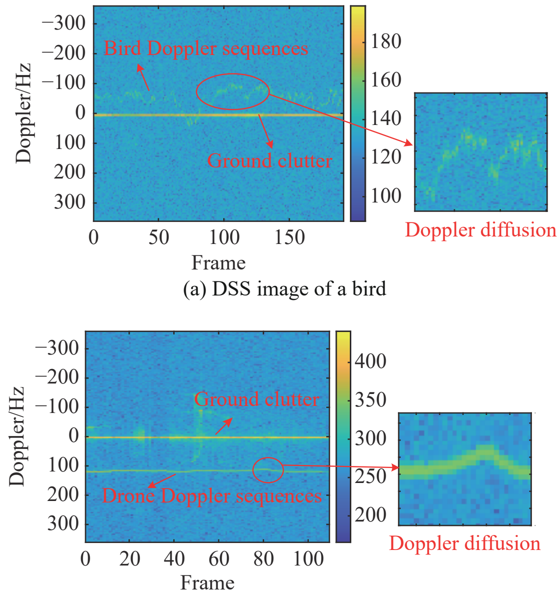

(a) DSS image of a bird

(b) DSS image of a drone

Fig. 1 Typical DSS images illustration

Table 1 Essential information for each Dopper signal

Symbol	Meaning	Extraction method
v_i	Relative velocity	Position of maximum value
A_i	Amplitude	Maximum value
N_i	Number of distributed points	CFAR
S_i	Sum of amplitudes	Sum of amplitudes of N_i points
a_i	Relative acceleration	Difference of relative velocity

Parameters in Table 1 are written in vector form to represent the behavior of the target in the ith frame. Suppose there are M frames. The time-related features can be written in a matrix for each DSS data as follows:

$$\boldsymbol{F}_a = \begin{bmatrix} \boldsymbol{v} \\ \boldsymbol{A} \\ \boldsymbol{N} \\ \boldsymbol{S} \\ \boldsymbol{a} \end{bmatrix} = \begin{bmatrix} v_1 & v_2 & \cdots & v_i & \cdots & v_M \\ A_1 & A_2 & \cdots & A_i & \cdots & A_M \\ N_1 & N_2 & \cdots & N_i & \cdots & N_M \\ S_1 & S_2 & \cdots & S_i & \cdots & S_M \\ a_1 & a_2 & \cdots & a_i & \cdots & a_M \end{bmatrix}. \tag{1}$$

To exploit the underlying periodical motions in the Doppler spectrum series, we manage to construct comprehensive and discriminative features using the information in Table 1. The constructed features can be divided into two main classes.

2.1 Target kinematic features

The proposed feature-based classification method utilizes kinematic features for classification since different targets possess different motion types. Human beings control drones for various tasks, whereas birds fly naturally by wing-beating [18]. These inherent features introduce different motion modulations to the recorded radar signals. Hence, several physical features are defined to describe their different motion patterns during observation. They are the mean velocity, the velocity variance, the mean acceleration, and the acceleration variance, which are respectively symbolized as μ_v, σ_v, μ_a, and σ_a.

Denote f_1 as the mean of the speed:

$$f_1 = \mu_t = \frac{1}{n}\sum_{t-1}^{n} v_i.$$

Denote f_2 as the variance of the velocity:

$$f_2 = \sigma_v = \frac{1}{n}\sum_{i=1}^{n}(v_i - u_v)^2.$$

Denote f_3 and f_4 as the mean and the variance of the acceleration respectively:

$$f_3 = \mu_a = \frac{1}{n-1}\sum_{t=1}^{n} a_t,$$

$$f_4 = \sigma_s = \frac{1}{n-1}\sum_{i=1}^{n}(a_i - \mu_s)^2.$$

2.2 Target RCS related features

Target RCS-related features are designed based on the underlying relationship between the RCS and the shape, size, and materials of targets. As stated in [18], in tracking individual released birds, the dominant RCS feature exhibits high repetitiveness which is almost sinusoidal with short breaks. Given this property, we design the periodic amplitude features to catch the character.

Firstly, the target energy ratio is the ratio of the maximum amplitude to the sum of total amplitudes of the target, namely $R_t = A_i / S_i$. This feature describes the centralization of target energy, which represents the micro-Doppler degree of the target. The proposed feature-based classification method uses its mean and variance for classification.

Denote f_5 and f_6 as the mean and the variance of the changing micro-Doppler degree with time respectively:

$$f_5 = \mu_R = \frac{1}{n}\sum_{i=1}^{n} R_i,$$

$$f_6 = \sigma_R = \frac{1}{n}\sum_{i=1}^{n}(a_R - \mu_R)^2.$$

Since RCS exhibits a sinusoidal curve, discrete cosine transform (DCT) is applied to R_i ($i = 1,2,\cdots,n$). The DCT of the energy ratio sequences is defined in [19,20] as follows:

$$\begin{cases} G_n(0) = \dfrac{\sqrt{2}}{n}\displaystyle\sum_{i=1}^{n} R_i \\ G_n(k) = \dfrac{2}{n}\displaystyle\sum_{i=1}^{n} R_i \cos\dfrac{(2n+1)k\pi}{2n} \\ k = 1,2,\cdots,n-1 \end{cases} \tag{2}$$

where $G_R(k)$ is the k th DCT coefficient. Based on the coefficients, the period of the sinusoidal and its ratio are defined.

The rearranged coefficients sequence $G'_R(k)$ is extracted after sorting the DCT coefficients in descending range. The period and its energy ratio feature are expressed as follows.

Denote f_7 as the relative period of Doppler variances:

$$f_7 = T_R = \frac{T(G'_R(1))}{n}$$

where $T(G'_R(1))$ means the period of the corresponding component.

Denote f_8 as the ratio of the amplitude of the central periodic part of the target:

$$f_8 = E_R = \frac{G'_R(1)}{G'_R(0)}.$$

The feature vector is constructed to represent the time-variant of the DSS image by writing the above features into vector forms. Given the extracted features, the posterior probability of each class is calculated. The classification is assigned to the possibility with the highest chance. For clarity, Fig. 2(a) shows the flowchart of the naive Bayes (NB) classifier with the extracted feature.

3. LSTM classifier construction

In this section, we construct LSTM architectures to realize classification. In recent years, it has been one of the state-of-the-art models for sequential data learning problems [21−25].

Unlike traditional speech and image signals, radar signals always suffer from high noise, clutter, and interference. As shown in Fig. 1, the ground clutter is several times stronger than the signal of targets. Therefore, preprocessing is recommended before feeding data into the network. The preprocessing progress is listed as follows.

Firstly, the ground clutter is removed by setting units around zero Doppler to zero as the ground clutter is static.

Afterward, the target Doppler units can be extracted by finding Doppler units around the peak position of the Doppler spectrum. In our experiment, the total number of units is 100, according to its resolution.

After preprocessing, the extracted Doppler units at each moment are fed into the LSTM classification network to train and test them. We build the LSTM network as shown in Fig. 2(b). Firstly, this network uses the bidirectional LSTM (Bi-LSTM). Afterward, 100 hidden units in the forward and backward sequence LSTMs are created, followed by a fully-connected layer with two outputs. Finally, the Softmax layer solves the classification problem. The loss function is

$$L(\theta) = -\frac{1}{C}\sum_i y_i \ln(\hat{y}_i) \tag{3}$$

where C is the number of the target classes, y is the one-hot representation of the ground truth, and $\hat{y}$ is the estimated probability.

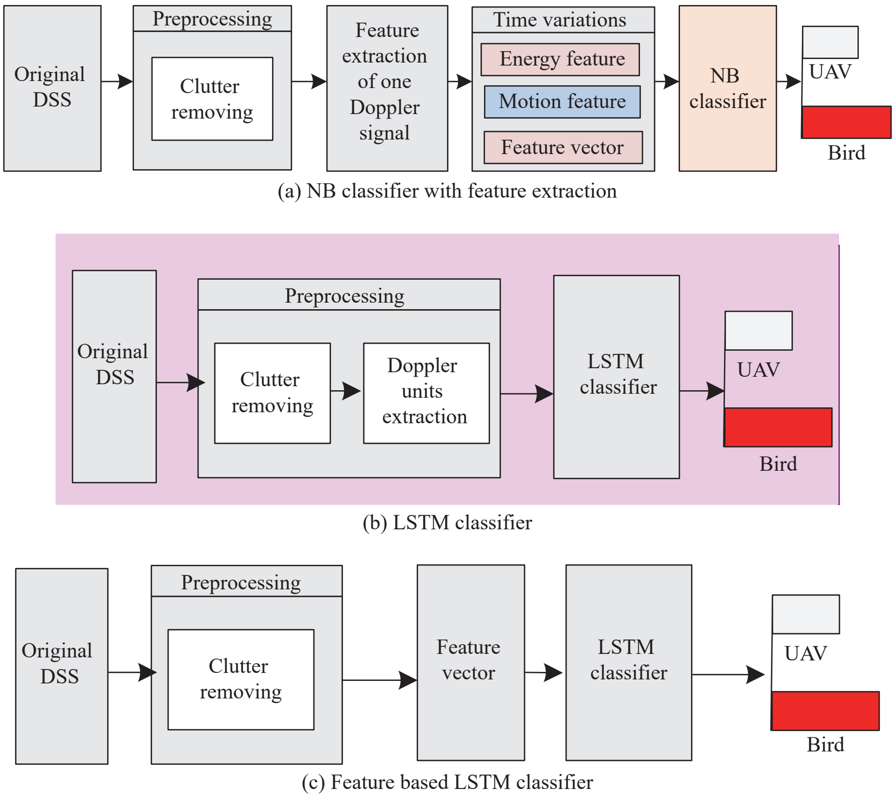

Fig. 2 Basic flowcharts of three classifiers with Doppler spectrum series

The LSTM is expected to work well in predefined circumstances, as LSTM is not good at extracting representative features of the signal, despite its superiority at learning complex dependencies across time. Therefore, its performance is highly related to the quality of the input signal.

To overcome this problem, we propose another scheme that feeds the extracted features of each Doppler spectrum as inputs instead of the extracted Doppler units. We use the feature vector in (1) as input. In this way, the size of the network decreases and the robustness is improved. Fig. 2(c) illustrates the architecture for classifying birds and drones based on the Doppler feature series. Compared with the LSTM classifier, it compresses each Doppler spectrum into five features.

As discussed above, we try to exploit the time-dependent property of the Doppler spectrum to discriminate drones from birds. We propose three typical structures which represent most mainstream time-variant property-based classification methods. For clarity, they are named the handcrafted feature classifier, the LSTM classifier, and the feature-based LSTM classifier.

4. Experiments and analysis

This section provides validation for utilizing the Doppler spectrum sequences for small radar target classification through measured data experiments. We explore the significant factors affecting the classification performances of three proposals based on the defined criteria.

4.1 Dataset and preprocessing

The measured data in this paper is collected with radar operating in the L band with 1.36 GHz central frequency.

The drones considered for classification are the DJI Drone Phantoms. With heights varying from 20 m to 50 m, distances ranging from 1 km to 4 km, and velocities from 2 m/s to 10 m/s, 23 tracks are recorded, with 15 tracks for birds and eight for drones. As we exploit the different periodical motions of targets for classification, it is essential to find sufficient observed frames for correct sorting. Therefore, we cut the above tracks into eight sets, with a minimum of four frames to a maximum of 32 frames. The interval is set as 4. The training data set is constructed by randomly selecting eight tracks for birds and four for drones. When the number of frames is more than 16, tracks are departed with half overlap to promise the dimension. The dimensions of the training tracks and the testing tracks are listed as follows.

(i) Four frames per track: 1 118 training tracks and 444 testing tracks.

(ii) Eight frames per track: 834 training tracks and 231 testing tracks.

(iii) 12 frames per track: 564 training tracks and 156 testing tracks.

(iv) 16 frames per track: 828 training tracks and 228 testing tracks.

(v) 20 frames per track: 675 training tracks and 186 testing tracks.

(vi) 24 frames per track: 546 training tracks and 141 testing tracks.

(vii) 28 frames per track: 474 training tracks and 123 testing tracks.

(viii) 32 frames per track: 405 training tracks and 102 testing tracks.

We use traditional evaluation criteria, such as the confusion matrix, accuracy, precision, and recall rates. The confusion matrix gives an overall classification result. In the confusion matrix, the number of each type of prediction is given. The accuracy is defined as (TP + TN)/(TP + FN + FP + TN) to assess the classification of the whole class, where, TP means the drone sample predicted as a drone, FN means the drone sample predicted as a bird, FP means a bird predicted as a drone, and TN is a bird prediction as a bird. The precision is defined as TP/(TP + FP). The recall rate is defined as TP/(TP + FN). The precision and recall criteria are used to evaluate the performance of the classifier on drone identification.

4.2 Performance versus frame number

This subsection presents experiments to validate the effectiveness of exploiting the DSS data for classification. Furthermore, the dependency of frame numbers is discussed through experimental results.

Firstly, experiments are conducted with the above dataset and their criteria with the frame number shown in Fig. 3. As Fig. 3 shows, the handcrafted feature classifier is independent of the frame number. At the same time, LSTM-based methods perform better with more frames. When the frame number is more than 16, the LSTM classifier outperforms the handcrafted classifier. However, for the feature-based LSTM classifier, the number is 20 to outperform the handcrafted classifier. This phenomenon is beneficial to the high quality of long-time dependence extraction of LSTM architectures. With different performances, all proposed methods can discriminate drones from birds at a high rate, proving the effectiveness of utilizing DSS data for classification.

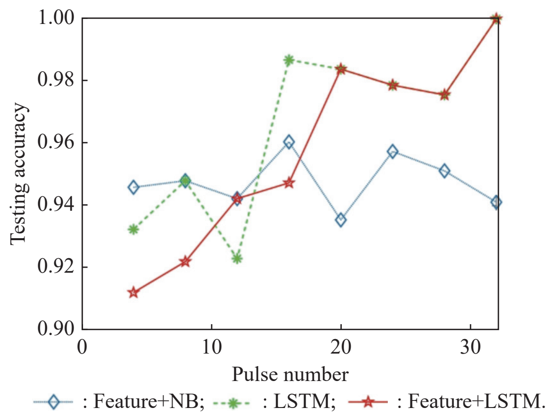

Fig. 3 Comparison of accuracy curves

For clarity, Fig. 4 illustrates the computed confusion matrix. As Fig. 4 shows, the proposed feature-based LSTM classifier has a better precision rate than the other two methods, even with lower accuracy at short-time observations. Moreover, the LSTM classifier performs better than the handcrafted feature method when the observation time is not shorter than 16 frames.

		Feature+NB classifier		LSTM classifier		Feature+LSTMclassifier	
		Drone	Bird	Drone	Bird	Drone	Bird
Pulse number=4	Drone	195/92.9%	9/3.8%	183/87.1%	3/1.3%	207/98.6%	36/15.4%
	Bird	15/7.1%	225/96.2%	27/12.9%	231/98.7%	3/1.4%	198/84.6%
Pulse number=8	Drone	96/88.9%	0/0%	96/88.9%	0/0%	105/97.7%	15/12.2%
	Bird	12/11.1%	123/100%	12/11.1%	123/100%	3/2.3%	108/87.8%
Pulse number=12	Drone	63/87.5%	0/0%	60/83.3%	0/0%	72/100%	9/10.7%
	Bird	9/12.5%	84/100%	12/16.7%	84/100%	0/0%	75/89.3%
Pulse number=16	Drone	96/91.4%	0/0%	102/88.9%	0/0%	105/100%	12/9.8%
	Bird	9/8.6%	123/100%	12/11.1%	123/100%	0/0%	111/90.2%
Pulse number=20	Drone	75/86.2%	0/0%	84/96.6%	0/0%	87/100%	3/3%
	Bird	12/13.8%	99/100%	3/3.4%	99/100%	0/0%	96/97%
Pulse number=24	Drone	60/90.9%	0/0%	63/95.5%	0/0%	66/100%	3/4%
	Bird	6/9.1%	75/100%	3/4.5%	75/100%	0/0%	72/96%
Pulse number=28	Drone	51/89.5%	0/0%	54/94.7%	0/0%	57/100%	3/4.5%
	Bird	6/10.5%	66/100%	3/5.3%	66/100%	0/0%	63/95.5%
Pulse number=32	Drone	45/88.2%	0/0%	51/100%	0/0%	51/100%	0/0%
	Bird	6/11.8%	51/100%	0/0%	51/100%	0/0%	51/100%

Fig. 4 Comparison of confusion matrix

4.3 Performance under different circumstances

In this subsection, we try to explore the factors affecting the performance of our proposals. Firstly, we add different Gaussian distributed noise to the original dataset to simulate diverse SNR circumstances. Under each SNR, Monte Carlo experiments are carried out 50 times to assess their performance solidly. Afterward, to give an overall assessment, we augment the dataset. Half of the data is augmented with random Doppler shifting ranging from −50 to 50 units, and the remaining half with noise addition.

(i) Performance in different SNR circumstances

Different Gaussian distributed noise signals are added to the original dataset to generate datasets with different SNRs ranging from −10 dB to 10 dB with a 5 dB interval. The Monte Carlo experiments are repeated 50 times for each SNR, considering the randomly changed noise.

The testing accuracy curves under different SNRs are plotted in Fig. 5. As we can see from the plots, the performances degrade with decreasing SNRs, especially for the LSTM classifier compared with the other two methods. Under low SNRs, the performance of the handcrafted feature classifier and the feature-based LSTM classifier are similar. With increasing SNRs, the feature-LSTM classifier outperforms the handcrafted feature one.

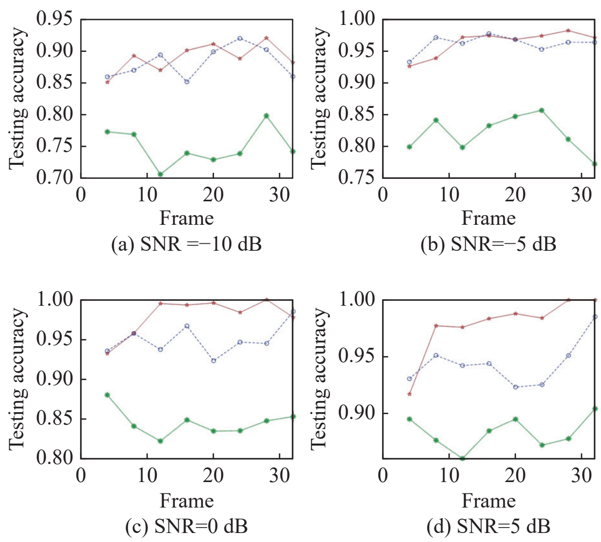

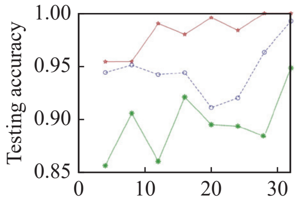

(e) SNR=10 dB

: LSTM; : Feature+NB; : Feature+LSTM.

Fig. 5 Accuracy curves under different SNRs

Moreover, the superiority becomes more evident with increasing SNRs. When SNR is higher than 0 dB, the feature-based LSTM classifier outperforms the other two methods, with a more significant frame than 12. The feature-based LSTM classifier tends to perform better with longer frames. At the same time, this tendency of the LSTM classifier begins to make a difference when the SNR is as high as 10 dB.

(ii) Data augmentation

In this experiment, we augment our dataset. First, we randomly select half of the data and add random Doppler shifts ranging from −50 to 50 units. Afterward, remained half of the dataset is added with random Gaussian distributed noise ranging from 0 dB to 20 dB. The confusion matrix is illustrated in Fig. 6. For clarity, the accuracy rate, precision rate, and recall rate are also plotted in Fig. 7. As we can see from Fig. 7, the feature-based LSTM classifier outperforms the other two methods, under the circumstances with Doppler shifts and serious noise, due to its robustness to environments. Even when the frame number is small, its performance is ideal. The performance is improved with increasing frame number as well. Moreover, it owns the highest precision rate among the three methods, which may benefit from the captured law of feature changing with the time of drones.

		Feature+NB classifier		LSTM classifier		Feature+LSTMclassifier	
		Drone	Bird	Drone	Bird	Drone	Bird
Pulse number=4	Drone	389/92.6%	20/4.3%		397/94.5%	402/95.7%	14/3%
	Bird	31/7.4%	448/95.7%		23/5.5%	18/4.3%	454/97%
Pulse number=8	Drone	191/88.4%	0/0%		184/85.2%	207/95.8%	0/0%
	Bird	25/11.6%	246/100%		32/14.8%	9/4.2%	246/100%
Pulse number=12	Drone	126/87.5%	0/0%		117/81.3%	144/100%	0/0%
	Bird	18/12.5%	168/100%		27/18.%	0/0%	168/100%
Pulse number=16	Drone	191/91%	0/0%		187/89%	209/99.5%	0/0%
	Bird	19/9%	246/100%		23/11%	1/0.5%	246/100%
Pulse number=20	Drone	145/83.3%	0/0%		163/93.7%	174/100%	4/2%
	Bird	29/16.7%	198/100%		11/6.3%	0/0%	194/98%
Pulse number=24	Drone	121/91.7%	0/0%		117/88.6%	132/100%	0/0%
	Bird	11/8.3%	150/100%		15/11.4%	0/0%	150/100%
Pulse number=28	Drone	102/89.5%	1/0.7%		96/84.2%	114/10%	1/0.7%
	Bird	12/10.5%	131/99.3%		18/15.8%	0/0%	131/99.3%
Pulse number=32	Drone	99/97.1%	1/1%		87/85.3%	102/100%	3/3%
	Bird	3/2.9%	101/99%		15/14.7%	0/0%	99/97%

1

0

Fig. 6 Confusion matrix comparison

The handcrafted feature classifier and the LSTM classifier share similar performance. Although their performances are not as good as the feature-based LSTM classifier, they are acceptable. These results validate the effectiveness of exploiting the DSS data to classify drones and birds.

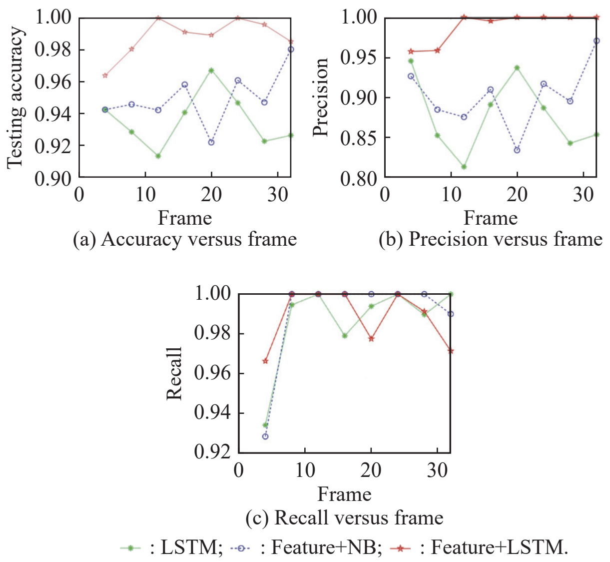

Fig. 7 Criteria variation with frame number

Through the above experiments, the following conclusions can be drawn.

(i) It is feasible to exploit DSS data to classify birds and drones, even with short observations.

(ii) The handcrafted feature classifier is suitable for shorter observed frames and low SNR. We recommend the LSTM classifier with increasing observed frames in high SNR cases. The feature-based LSTM classifier best suits low SNR circumstances.

(iii) Regarding the varieties such as Doppler shifts introduced in the testing data, both the handcrafted feature-based classifier and the feature-based LSTM classifier are better choices. With increasing SNR and frame number, the feature-based LSTM classifier is the most suitable method.

(iv) The feature-based LSTM classification is best suited for drone discrimination and detection tasks.

5. Conclusions

This paper proves the effectiveness of utilizing DSS data to discriminate drones from birds. We propose three schemes according to the existing mainstream classification methods. The handcrafted feature-based classification is most stable by extracting micromotion features and tracking features jointly without micro-Doppler detecting progress. By feeding the LSTM with preprocessed data and feature vector sequences, we propose the LSTM classification method and the feature-based LSTM classification method to exploit the underlying differences in periodic motions of birds and drones. Through experiments, we prove the effectiveness of three proposed methods. The proposed method requires a high Doppler resolution to catch the Doppler diffusions. Although experimental results can validate the effectiveness of the proposed method. We believe a dataset with more abundant classes and track numbers will improve our research and bring about more interesting work.

Acknowledgment

The authors would like to thank The Pearl River Talent Recruitment Team for their data approval.

References

[1] LACHER A R, ZEITLIN A, MARONEY D R, et al. Airspace integration alternatives for unmanned aircraft. Proc. of the AUVSI’s Unmanned Systems Asia-Pacific, 2010: 10-0090.

[2] YU X Y, ZHU Y, QIU L X, et al. Energy efficient offloading strategy for UAV aided edge computing systems. Systems Engineering and Electronics, 2022, 44(3): 1022–1029. (in Chinese)

[3] ZENG Y, ZHANG R, LIM T J, Wireless communications with unmanned aerial vehicles: opportunities and challenges. IEEE Communications Magazine, 2016, 54(5): 36–42.

[4] MOTLAGH N H, BAGUA M, TALEB T. UAV-based IoT platform: a crowd surveillance use case. IEEE Communications Magazine, 2017, 55(2): 128–134.

[5] RAHMAN S, ROBERTSON D A. Classification of drones and birds using convolutional neural networks applied to radar micro-Doppler spectrogram images. IET Radar, Sonar & Navigation, 2020, 14(5): 653–661.

[6] HUIZING A, HEILIGERS M, DEKKER B, et al. Deep learning for classification of mini-UAVs using micro-Doppler spectrograms in cognitive radar. IEEE Aerospace and Electronic Systems Magazine, 2019, 34(11): 46–56.

[7] BJORKLUND S, WADSTROMER N. Target detection and classification of small drones by deep learning on radar micro-Doppler. Proc. of the International Rader Conference, 2019: 19573428.

[8] RITCHIE M, FIORANELLI F, BORRION H, et al. Multistatic micro-Doppler radar feature extraction for classification of unloaded/loaded micro-drones. IET Radar, Sonar & Navigation, 2017, 11(1): 116–124.

[9] KANG K B, CHOI J H, CHO B L, et al. Analysis of micro-Doppler signatures of small UAVs based on Doppler spectrum. IEEE Trans. on Aerospace and Electronic Systems, 2021, 57(5): 3252–3267.

[10] LI T M Y, WEN B Y, TIAN Y W, et al. Numerical simulation and experimental analysis of small drone rotor blade polarimetry based on RCS and micro-Doppler signature. IEEE Antennas and Wireless Propagation Letters, 2019, 18(1): 187–191.

[11] GONG J K, YAN J, LI D, et al. Theoretical and experimental analysis of radar micro-Doppler signature modulated by rotating blades of drones. IEEE Antennas and Wireless Propagation Letters, 2020, 19(10): 1659–1663.

[12] TORVIK B, OLSEN K E, GRIFFITHS H. Classification of birds and UAVs based on radar polarimetry. IEEE Geoscience and Remote Sensing Letters, 2016, 13(9): 1305–1309.

[13] KIM B K, KANG H S, LEE S, et al. Improved drone classification using polarimetric merged-Doppler images. IEEE Geoscience and Remote Sensing Letters, 2021, 18(11): 1946–1950.

[14] ZHAN W J, YI J X, WAN X R, et al. Track-feature-based target classification in passive radar for low-altitude airspace surveillance. IEEE Sensors Journal, 2021, 21(8): 10017–10028.
[15] MOHAJERIN N, HISTON J, DIZAJI R, et al. Feature extraction and radar track classification for detecting UAVs in civilian airspace. Proc. of the IEEE Radar Conference, 2014: 674–679.
[16] TAHA B, SHOUFAN A. Machine learning-based drone detection and classification: state-of-the-art in research. IEEE Access, 2019, 7: 138669–138682.
[17] ROHLING H. Radar CFAR thresholding in clutter and multiple target situations. IEEE Trans. on Aerospace and Electronic Systems, 1983, AES-19(4): 608–621.
[18] VAUGHN C R. Birds and insects as radar targets: a review. Proceedings of the IEEE, 1985, 73(2): 205–227.
[19] AHMED N, NATARAJAN T, RAO K R. Discrete cosine transform. IEEE Trans. on Computers, 1974, C-23(1): 90–93.
[20] WALLACE G K. The JPEG still picture compression standard. IEEE Trans. on Consumer Electronics, 1992, 38(1): xviii–xxxiv.
[21] HOCHREITER S, SCHMIDHUBER J. Long short-term memory. Neural Computation, 1997, 9(8): 1735–1780.
[22] GREFF K, SRIVASTAVA R K. LSTM: a search space odyssey. IEEE Trans. on Neural Networks and Learning Systems, 2017, 28(10): 2222–2232.
[23] GERS F A, SCHMIDHUBER J, CUMMINS F. Learning to forget: continual prediction with LSTM. Neural Computation, 2000, 12(10): 2451–2471.
[24] JI R P, ZHANG C Y, LIANG L X, et al. Trajectory prediction of boost-phase ballistic missile based on LSTM. Systems Engineering and Electronics, 2022, 44(6): 1968–1976. (in Chinese)
[25] ALTMANN M, OTT P, STACHE N C, et al. Learning dynamic processes from a range-Doppler map time series with LSTM networks. Proc. of the 16th European Radar Conference, 2019: 13–16.

Biographies

DUAN Jia was born in 1989. She received her Ph.D. degree in signal processing from Xidian University in 2015. She worked for the Chinese Aviation Industry Corporation as a senior engineer in signal processing and target recognition from 2016 to 2021. Afterward, she works as an associate research fellow in the School of Electronics and Communication, Sun Yat-sen University. Her research interests include radar signal processing, ISAR imaging, SAR/ISAR feature extraction and target recognition.
E-mail: bifiduan119@126.com

ZHANG Lei was born in 1984. He received his B.S. degree from Chang 'an University in 2006. He received his Ph.D. degree from Xidian University in 2011. He worked in the National Key Lab of Radar Signal Processing from 2011 to 2019. Currently, he works as a professor in the School of Electronics and Communication, Sun Yat-sen University. His research interests include radar signal processing, SAR/ISAR imaging, SAR interpreting, electronic counter measures, etc.
E-mail: zhanglei57@mail.sysu.edu.cn

WU Yifeng was born in 1988. He received his B.S. and Ph.D. degrees from Xidian University in 2010 and 2016, respectively. He worked for the Chinese Aviation Industry Corporation as a senior engineer in signal processing and target detection from 2016 to 2020. Currently, He works as an associate professor in the School of Electronics and Communication, Sun Yat-sen University. His research interests include signal processing, space-time adaptive processing, radar target detection, and clutter suppression.
E-mail: wuyf95@mail.sysu.edu.cn

ZHANG Yue was born in 1980. He received his Ph.D. degree in electronic science and technology at National University of Defense Technology. He is now an associate professor in Sun Yat-sen University. His research interests include radar signal processing and automatic targets recognition.
E-mail: zhangyue_frog1@163.com

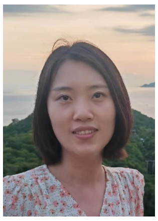

ZHAO Zeya received her M.S. degree in information engineering from Information Engineering University. She is now with Beijing Institute of Tracking and Transmission Technology. Her research interests include radar signal analysis and intelligence information processing.
E-mail: zzy_kelly@163.com

GUO Xinrong received her B.Sc. and M.Sc. degrees in radio science from Xidian University, Xian, China, in 2011 and 2014, respectively. She is currently a Lecturer with Armed police Engineering University, Xian, China. Her research interests include inverse synthetic aperture radar imaging and computational electromagnetics.
E-mail: rapgxr@163.com